Journal of Engineering Physics and Thermophysics, Vol. 72, No. 6, 1999

NUMERICAL SIMULATION OF A HYPERSONIC GAS FLOW PAST COSMIC BODIES DURING THEIR PASSAGE THROUGH DENSE ATMOSPHERIC LAYERS

V. E. Okunev and G. S. Romanov

UDC 533.06.011

The technique and results of calculation of a nonstationary hypersonic gas flow past cosmic bodies during their passage through dense atmospheric layers with account for radiative energy transfer in the multigroup spectral approximation are presented.

By some estimates, collision of asteroids and large comets with the earth is a rather rare phenomenon and occurs once in 200–300 years. The probability of fall of bodies with a diameter of 10 to 100 m to the earth is much higher and can lead to global disastrous consequences. From the aforesaid the need to study the processes accompanying the entry of large cosmic bodies into the atmosphere of the earth and other planets follows.

We consider in brief the basic phenomena occurring in the motion of meteoroids in the atmosphere [1]. Interaction of a meteoroid with molecules of the atmosphere (convective heat transfer) leads to heating of the meteoroid surface to high temperatures, melting, and then to evaporation. In front of a cosmic body moving at a hypersonic velocity a shock wave forms – a comparatively thin gas layer in which the pressure, density, and temperature change sharply and energy of translational motion of molecules of the incident flow changes over to internal energy of the gas. A shock-compressed layer filled with atmospheric gas and vapor of the meteoroid substance lies between the shock-wave front and the body. The temperature in this region is rather high due to nearly complete retardation of the incoming flow in the central portion of the frontal cross section. The most substantial changes in the interaction between the incoming flow and the meteoroid arise after formation of a strong shock wave when convective heat transfer is supplemented with radiative energy transfer of the compressed layer in front of the frontal surface of the body. The shock-compressed layer exerts a major effect on the motion of the body. It manifests itself in the form of retardation and destruction of the body and plastic deformation. The processes of destruction of the streamlined body are associated mainly with splitting-off of fragments of the substance under the action of tensile stresses – crushing – and phase transformations – melting and evaporation. A stagnation zone with a reciprocating-circulating flow with a reduced density and low velocities lies behind the streamlined body.

By the estimates of [2], the maximum pressure on the leading blunt nose of a body moving in the atmosphere of Mars at a velocity of 30–50 km/sec amounts to about 10 MPa. Even these relatively low pressures can lead to crushing of the body, since meteoroids are usually not monolithic. Destruction of the meteoroid will last as long as the aerodynamic loads producing stresses in the body exceed the ultimate strength of the substance. Crushing leads to a sharp, burst-like increase in the energy acquired by the cosmic body due to an increase in the effective surface, which absorbs radiation. As a result, the substance of the meteoroid is converted from a condensed phase to the gas phase, which actually can be considered to be a burst.

In what follows we study only one of the aspects of a hypersonic gas flow past cosmic bodies upon their entry into the atmospheric layers – the radiative gasdynamics of the flow.

Recently, practice has posed, besides traditional problems of gasdynamics, a number of new complex problems concerned with the study of plasma flows in the presence of radiation and external and intrinsic electromagnetic fields, flows past bodies of complex geometry, etc. Analytical investigation of these problems is

Academic Scientific Complex "A. V. Luikov Heat and Mass Transfer Institute," National Academy of Sciences of Belarus, Minsk, Belarus. Translated from Inzhenerno-Fizicheskii Zhurnal, Vol. 72, No. 6, pp. 1159-1168, November–December, 1999. Original article submitted October 19, 1998.

1062-0125/99/7206-1121$22.00

impossible in many cases, because it requires solution of nonlinear equations of hydrodynamics with complex boundary conditions. By virtue of this, numerical simulation of the phenomena is of great interest.

The system of differential equations of radiative gasdynamics describing the gas flow around a meteoroid upon its entry into the atmosphere, is written in the cylindrical coordinates as follows:

$$\frac{\partial \rho}{\partial t} + \operatorname{div}(\rho \mathbf{w}) = 0,$$

$$\frac{\partial \rho u}{\partial t} + \operatorname{div}(\rho u \mathbf{w}) = -\frac{\partial P}{\partial z},$$

$$\frac{\partial \rho v}{\partial t} + \operatorname{div}(\rho v \mathbf{w}) = -\frac{\partial P}{\partial r}, \tag{1}$$

$$\frac{\partial \rho E}{\partial t} + \operatorname{div}(\rho E \mathbf{w}) + \operatorname{div}(P \mathbf{w}) + \operatorname{div} \mathbf{S} = 0.$$

To close this system of equations we use the dependences

$$P = P(\rho, \varepsilon), \quad T = T(\rho, \varepsilon).$$

System (1) was solved by the method of large particles [3] in the computational region $OEFG$ (Fig. 1) with the following initial conditions in the region beyond the streamlined body:

$$u(z, r, 0) = u_0, \quad v(z, r, 0) = 0, \quad \rho(z, r, 0) = \rho_0(t), \quad \varepsilon(z, r, 0) = \varepsilon_0.$$

The boundary conditions were selected as follows:

on the Z axis

$$\frac{\partial P}{\partial r} = \frac{\partial \rho}{\partial r} = \frac{\partial E}{\partial r} = \frac{\partial u}{\partial r} = 0, \quad v(z, 0, t) = 0;$$

on the boundary OE

$$\frac{\partial P}{\partial z} = \frac{\partial \rho}{\partial z} = \frac{\partial E}{\partial z} = \frac{\partial u}{\partial z} = 0, \quad u(0, r, t) = u_0;$$

on the boundary of the computational region EF

$$\frac{\partial P}{\partial r} = \frac{\partial \rho}{\partial r} = \frac{\partial E}{\partial r} = \frac{\partial u}{\partial r} = \frac{\partial v}{\partial r} = 0;$$

on the boundary of the computational region FG

$$\frac{\partial P}{\partial z} = \frac{\partial \rho}{\partial z} = \frac{\partial E}{\partial z} = \frac{\partial u}{\partial z} = \frac{\partial v}{\partial z} = 0;$$

on the boundary of the body $ABCD$ nonflow conditions were set.

In the computational region $OEFG$ a rectangular grid was introduced; the dimensions of the cells along the Z axis and the radius R were chosen from the criterion of good convergence of the solution with a decrease in the spatial steps.

The surface of the streamlined body $ABCD$ evaporates under the action of thermal radiation of plasma. The boundary conditions on the surface were set according to the technique of [4].

A numerical solution of problems of radiative gasdynamics presents great difficulties even when using modern high-speed computers. The system of equations describing the dynamics of a radiating gas is much more complex than the equations of conventional gasdynamics. This is associated with the fact that the spectral intensity

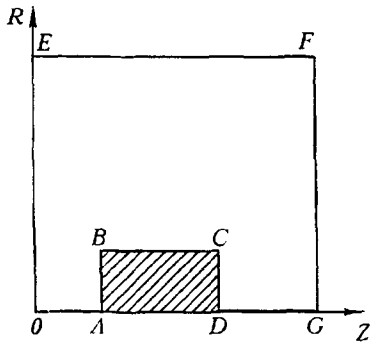

Fig. 1. Shape of the computational region.

of the radiation, which is a function of the frequency, the coordinate of the point, and the direction of radiation propagation, is used in the transfer equation. At the same time, only an integral characteristic of the field – the density of the radiation flow – enters the energy equation. By the most conservative estimates, the number of computational points required for the soution of two-dimensional problems of radiative gasdynamics amounts to about $2 \cdot 10^5$ (2000 points in space, 10 in angular directions, and 10 group intervals in the energy of quanta). Moreover, one should usually make 10^3-10^4 time steps, which is caused by the long persistence, from the gasdynamic viewpoint, of the process or by a desire to obtain more detailed temporal or spatial characteristics of the flow. Thus, it is seen that the solution of nonstationary problems of gasdynamics with account for radiative energy transfer is associated with a large volume of computational work and extremely large expenditures of computer time. Therefore, to simplify such problems we use one or another method of averaging the transfer equation with respect to the energy of photons and the angular distribution, which leads to a reduction in its dimensionality.

The density of the radiation flow entering the energy equation was found by solving the equation of radiation transfer according to the technique of [4].

Below we present results of calculations of a hypersonic air flow past a cylindrical body with a radius of 0.5 km upon its passage through dense layers of the atmosphere at a velocity of 50 and 10 km/sec. These velocities of entry of bodies into the atmosphere in the nonstationary case (with account for variable density and radiative transfer of energy in the multigroup spectral approximation) have not been considered in the literature. Numerical simulation of hypersonic flows past bodies without regard for the dynamics of body descent give qualitatively different results. In the first and second versions of the calculations passage of the body at a velocity of 50 and 10 km/sec through a nonuniform atmosphere from a height $H = 50$ km to $H = 15$ km above the earth's surface is studied. The standard atmosphere of CIRA of 1961 was used as the model of the atmosphere. In a third version we studied a uniform air flow past a cylindrical body of radius $R = 0.5$ km at a velocity $U = 50$ km/sec. The density of the incoming flow corresponded to $\rho = 1.02 \cdot 10^{-6}$ g/cm^3 at a height $H = 50$ km above the earth's surface.

The thermodynamic and optical characteristics of the incoming flow were simulated in the calculations by the actual properties of air [5]. The transfer equation was solved in the multigroup approximation (14 spectral groups). The boundaries of the spectral groups were chosen as follows: 1) 0.0015497–0.51142 eV, 2) 0.51142–1.4103 eV, 3) 1.4103–2.7121 eV, 4) 2.7121–4.5098 eV, 5) 4.5098–6.5244 eV, 6) 6.5244–7.9502 eV, 7) 7.9502–9.9649 eV, 8) 9.9649–18.612 eV, 9) 18.612–80.585 eV, 10) 80.585–247.95 eV, 11) 247.95–398.00 eV, 12) 398.00–2300 eV, 13) 2300–6000 eV, 14) 6000–20,000 eV.

In numerical realization of the technique of the calculations, the equations of state of air and the spectral coefficients of absorption were specified in tables in the form of the logarithms of the corresponding quantities with a uniform logarithmic step over the variables used. The values of the quantities were found by linear interpolation.

The hypersonic gas flow past a meteoroid was calculated on a rectangular computational grid *OEFG* (Fig. 1) containing 4150 cells. Fifty computational cells were taken along the radius R and 83 cells along the symmetry axis Z. Since in these calculations, we were mainly interested in the flow in front of the streamlined body, only a few cells were taken along the Z axis behind the frontal surface AB. To describe the shock-compressed region in front of the streamlined body in more detail, the spatial steps were selected as follows: in front of the body the

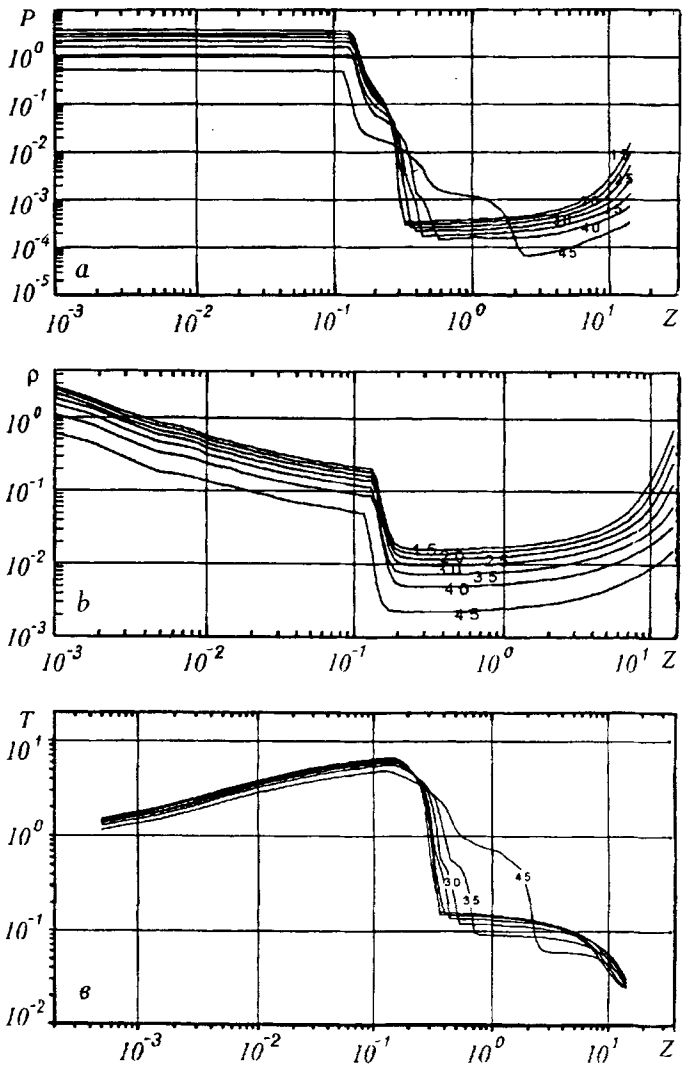

Fig. 2. Profiles of pressures (a), densities (b), and temperatures (c) for various heights above the surface. P, 10 MPa; ρ, kg/m^3; T, eV; Z, km.

step along the Z axis was taken to be $\Delta Z_0 = 1$ m, and then its size was increased ($\Delta Z_{i+1} = \Delta Z_i a_z$). The first 25 cells along the R axis were of the same length $\Delta R_0 = 20$ m, and then the size of the spatial step along the coordinate R was increased ($\Delta R_{j+1} = \Delta R_j a_r$, where a_z and a_r are factors that can be varied). We took the following values of these factors: $a_z = 1.095$ and $a_r = 1.1$. Thus, the computational grid along the Z axis and along the radial direction amounted to 15 km and 2.45 km, respectively.

In numerical simulation of a two-dimensional gas flow past bodies problems associated with optimum choice of the computational grid arise. On the one hand, the limited resources of computers do not allow calculations on detailed spatial grids, and on the other, calculation of the flow on small grids can introduce substantial errors. The problem of a high-velocity gas flow past a meteoroid has its own specific properties: the presence of a relatively narrow zone of shock-compressed gas adjacent to the frontal surface. The length of this zone amounts to only 15–20% of the diameter of the streamlined body. This narrow compressed layer is of most interest in the study of hypersonic gas flows past bodies. A heated layer formed due to absorption of hard quanta of radiation, emitted from the shock-wave front, by cold air lies in front of the shock-compressed layer. The length of the heated layer may be rather large compared to the thickness of the shock-compressed region, especially at large heights, where the density of the surrounding atmosphere is low and the path lengths of the radiation, conversely, reach large values. In order to allow for these special features of the flow past a meteoroid, the computational grid is compressed near the body. Far from the shock-compressed layer the size of the cells of the computational grid is increased, thus making it possible to cover a large computational region.

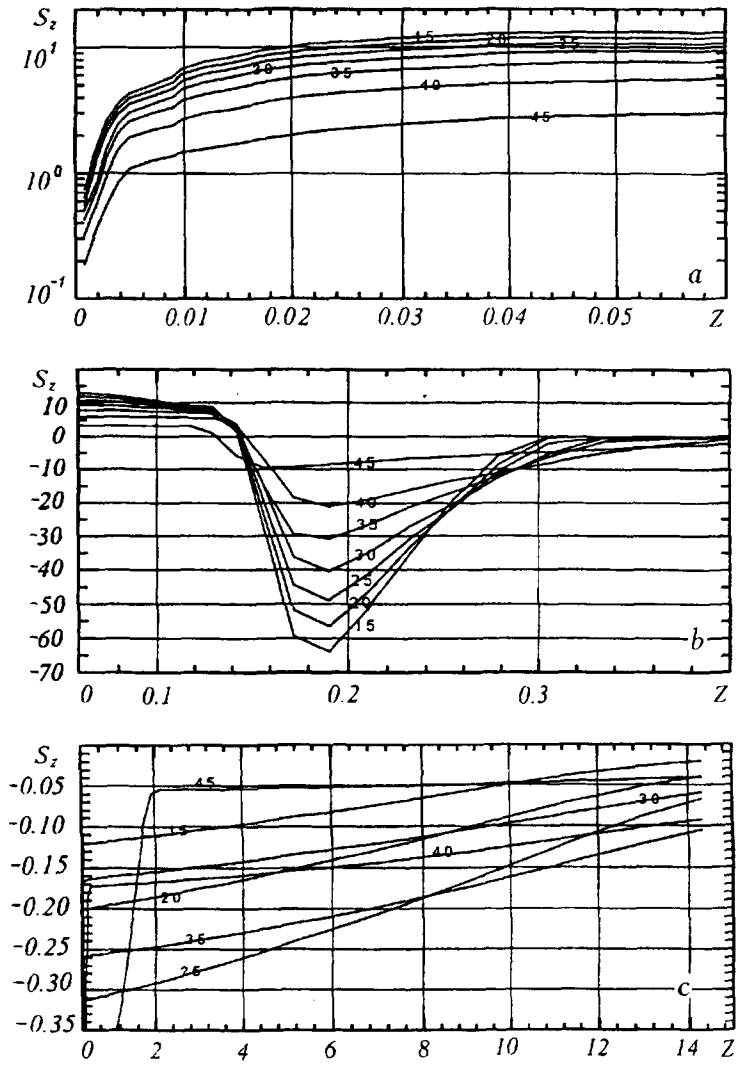

Fig. 3. Distribution of the radiative flow density along the axis for $0 \leq Z \leq 0.06$ km (a), $0.06 \leq Z \leq 0.4$ km (b), and $0.4 \leq Z \leq 15$ km (c). S_z, MW/cm^2.

The pattern of the flow past a body is the following. Upon entry of the meteoroid into the atmospheric layers at a hypersonic velocity, a shock wave is formed in front of it, passing through which the gas flow is retarded. Kinetic energy of the gas changes over to internal energy. In this case, the density, pressure, and temperature of the gas increase sharply. A shock-compressed layer of plasma is formed in front of the frontal surface of the meteoroid. At large velocities of entry of the body into the atmosphere the temperature in the shock-compressed layer reaches high values. The radiative flow from the shock-compressed layer for moderate heights ($H < 50$ km) at hypersonic velocities of the flow past the body ($V \geq 10$ km/sec) greatly exceeds the convective flow [6]. Under the action of the radiative flow generated by the shock-compressed layer, the surface of the meteoroid begins to heat up and then to evaporate. The boundary layer consisting of streamlining gas is pushed away from the frontal surface by gaseous products of evaporation. Here, the layer of gaseous products of meteoroid ablation considerably weakens the radiative flow incident on the body. Radiation emitted from the shock-compressed layer heats cold air layers lying in front of the shock-wave front mainly due to shortwave quanta of light. Only longwave quanta of radiation in the visible and IR spectral regions go to infinity.

Figure 2 presents distributions of pressure, density, and temperature along the Z axis (reckoned from the body surface) for the first version of calculation (an inflow velocity $U = 50$ km/sec). The figures at the curves indicate distributions of the corresponding quantities along the Z axis for various heights above the earth's surface. In the first and second versions, the departure of the shock wave from the body almost does not change with the

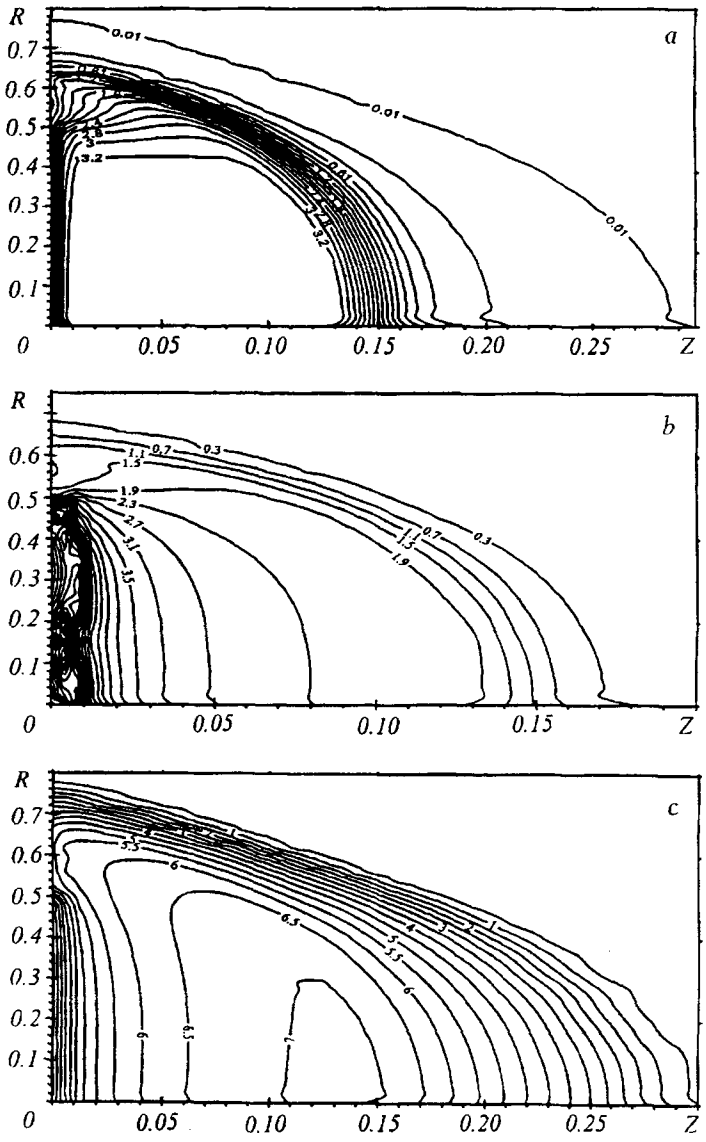

Fig. 4. Isolines of pressures (a), densities (b), and temperatures (c). P, 10 MPa; ρ, 10^{-4} g/cm^3; T, eV; R, km.

height of the streamlined body and amounts to about 140 m. In the shock-compressed layer the pressure remains virtually constant over the layer thickness. Thus, at a height H = 15 km, the pressure in the shock-compressed layer reaches a value equal to 361 atm, whereas in front of the shock wave it is $3.36 \cdot 10^{-2}$ atm. The density in front of the shock wave is $1.57 \cdot 10^{-5}$ g/cm^3, and behind the shock-wave front it acquires a value of $2.07 \cdot 10^{-4}$ g/cm^3. Then the density increases, reaching a maximum value of $2.94 \cdot 10^{-3}$ g/cm^3 directly at the frontal surface of the streamlined body. At a height H = 15 km the maximum temperature behind the shock-wave front is 6.8 eV at Z = 140 m.

As the height of the meteoroid above the earth's surface decreases and, consequently, the density of the incoming flow and the temperature in the shock layer increase, the role of radiative flows grows due to an increase in the optical thickness of the compressed layer. Figure 3 shows the distribution of the radiative flow density along the Z axis as a function of the height above the earth's surface. Thus, the radiative flow at a height H = 15 km takes a maximum value of 64 MW/cm^2 at Z = 0.19 km (Fig. 3b). As is shown by the calculations, at a body height H = 15 km and a velocity of streamlining U = 50 km/sec, a radiative flow of about 0.7 MW/cm^2 falls onto the body. Under the action of it the body is heated and then begins to evaporate. A layer of gaseous products of evaporation is formed in front of the frontal surface of the meteoroid. The temperature of the body surface reaches 0.34 eV. Vapors flow into the region between the shock wave and the frontal surface at a velocity of 0.51 km/sec. Their

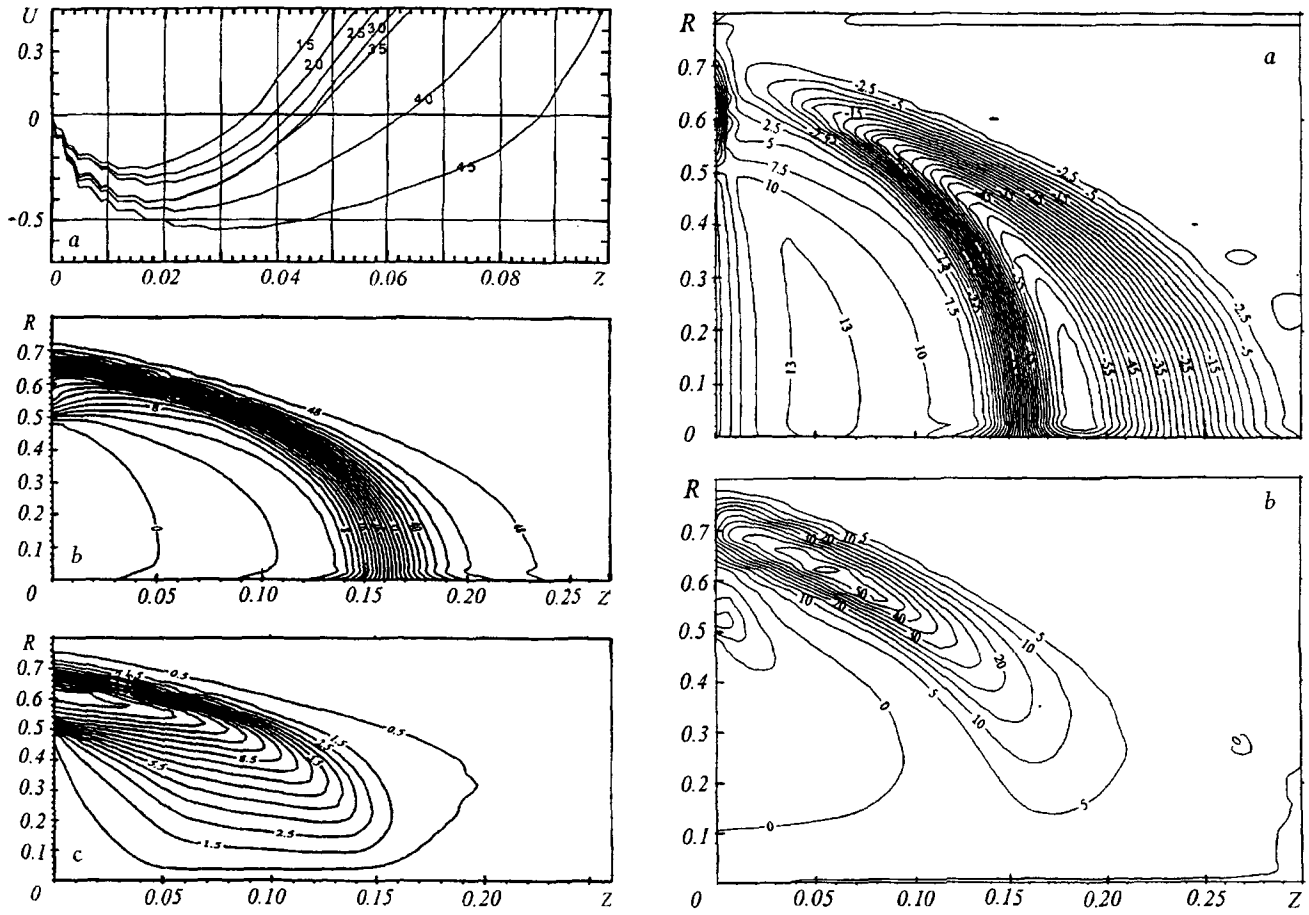

Fig. 5. Axial component of the velocity (a), isolines of axial components of the velocity (b), and isolines of radial components of the velocity vector (c). U, V, km/sec.

Fig. 6. Isolines of the axial (a) and radial (b) component of the radiative flow density. S_z, S_r, MW/cm^2.

density corresponds to a value of $5.5 \cdot 10^{-4}$ g/cm^3. For a height H = 15 km, the thickness of the region occupied by the vapors is 35 m. Radiation is strongly absorbed upon passing through the layer of gaseous products of evaporation. Thus, the radiative flow at the contact boundary (separating the evaporated substance and the air) lying a distance of 35 m from the body is about 12 MW/cm^2, and only 0.7 MW/cm^2 falls onto the body (Fig. 3a), with the largest contribution to the radiative flow being made by the fourth, fifth, and sixth spectral groups. The radiative flow reaching infinity corresponds to a value of 15.4 kW/cm^2 for H = 15 km. Here, the main contribution is made by the second (66%) and third (about 30%) spectral groups (the first version, a height above the earth's surface H = 15 km).

Figures 4-6 present two-dimensional fields of pressure, density, temperature, axial and radial components of the velocity, and axial and radial components of the density of the radiative flow.

For comparison, Fig. 7 presents distributions of pressure, density, and temperature along the Z axis for the second version (an incident flow velocity U = 10 km/sec). The figures at the curves indicate heights above the earth's surface. The maximum pressure and density for a height H = 15 km are reached near the frontal surface of the body and are 196 atm and $2.98 \cdot 10^{-3}$ g/cm^3, respectively. The highest temperature behind the shock-wave front is 1.21 eV. We note here that in the second version of the calculations the density behind the shock-wave front is distributed more uniformly, and the temperature is much lower. The total radiative flow falling on the body is 0.124 MW/cm^2. The largest contribution to it is made by the second (6.4%), third (22.7%), fourth (34.7%), fifth (23.3%), sixth (7.2%), and seventh (3.9%) spectral groups.

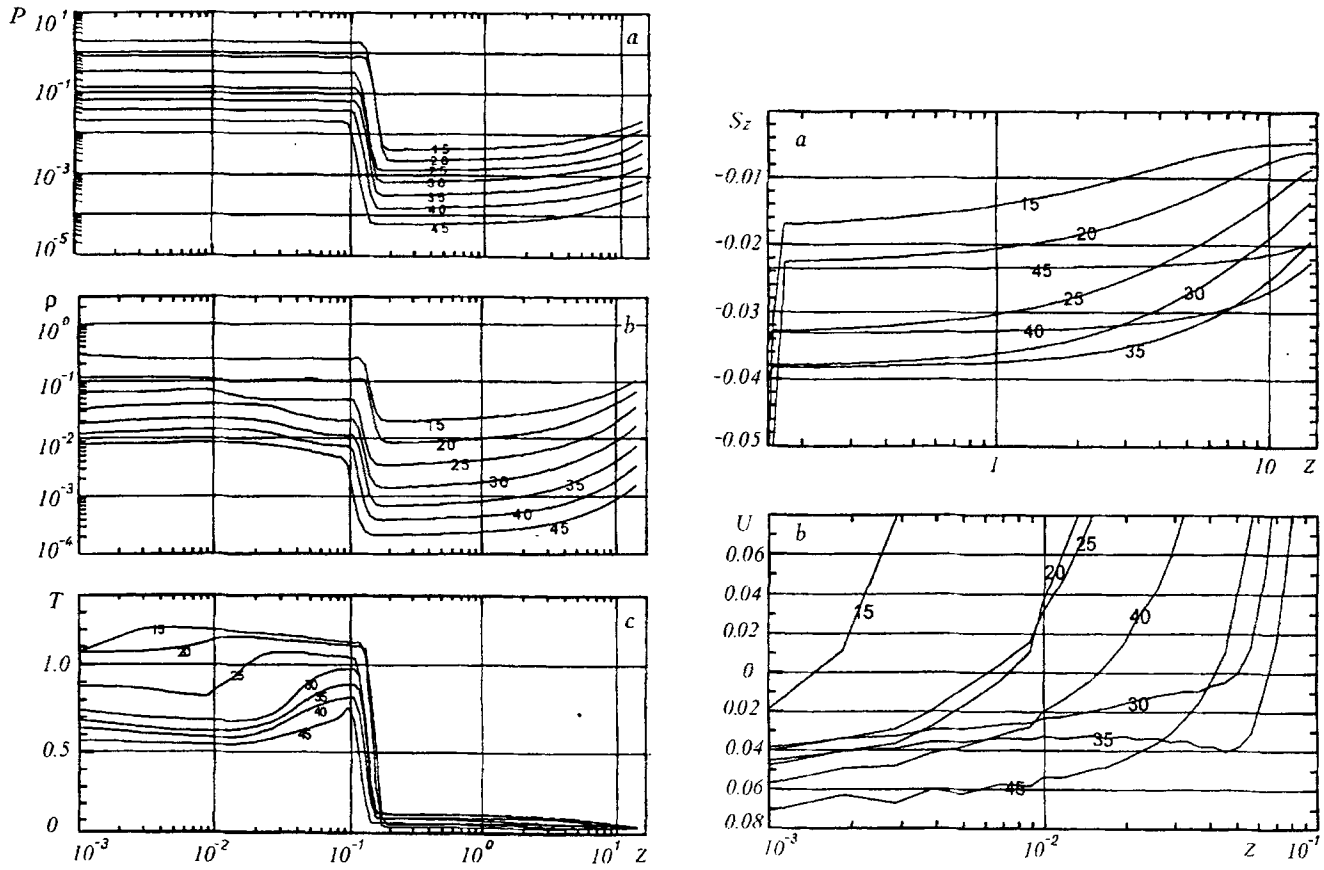

Fig. 7. Distribution of pressure, density, and temperature along the Z axis. P, 10 MPa; ρ, 10^{-2} g/cm^3; T, eV (second version).

Fig. 8. Axial components of the radiative flow density (a) and velocity (b) (second version).

The body surface is heated to a temperature of 0.33 eV. The density of the vapors entering the shock-compressed layer is $3 \cdot 10^{-4}$ g/cm^3, and their velocity is 0.49 km/sec. Figure 8a presents the distribution of the axial component of the total density of the radiative flow along the Z axis. The figures at the curves correspond to the height of the body above the earth's surface. As is seen from the figure, the total outgoing density of the radiative flow at the Z axis is 4.64 kW/cm^2, with the main contribution to the radiation being made by the second spectral group (99.6%).

Figure 8b shows the distribution of the axial component of the velocity vector. As the meteoroid approaches the denser layers of the atmosphere, the region occupied by gaseous products of evaporation decreases in width and lies closer to the frontal surface.

Figure 9 presents two-dimensional fields of temperature, density, and the radial component of the radiative flow density for the third version of the calculations (a uniform air flow past a cylindrical body with a flow density of $1.02 \cdot 10^{-6}$ g/cm^3, corresponding to a height of 50 km, and a velocity of 50 km/sec).

It is seen from the temperature curve that the heated layer is about 12 km at $R = 0.5$ km and about 8 km on the Z axis. This distribution of the length of the heated layer is attributed to flow nonuniformity near the meteoroid.

It is seen from Fig. 9b that the density near the symmetry axis is about twofold higher than at $R = 0.5$ km. By virtue of this the optical thickness of air near the axis is higher and radiation is absorbed at a smaller distance, thus leading to a smaller length of the heated layer.

The numerical simulation allowed one to present a picture of nonstationary hypersonic flow around a meteoroid. Detailed two-dimensional fields of gasdynamic parameters of the gas flow past a meteoroid are obtained.

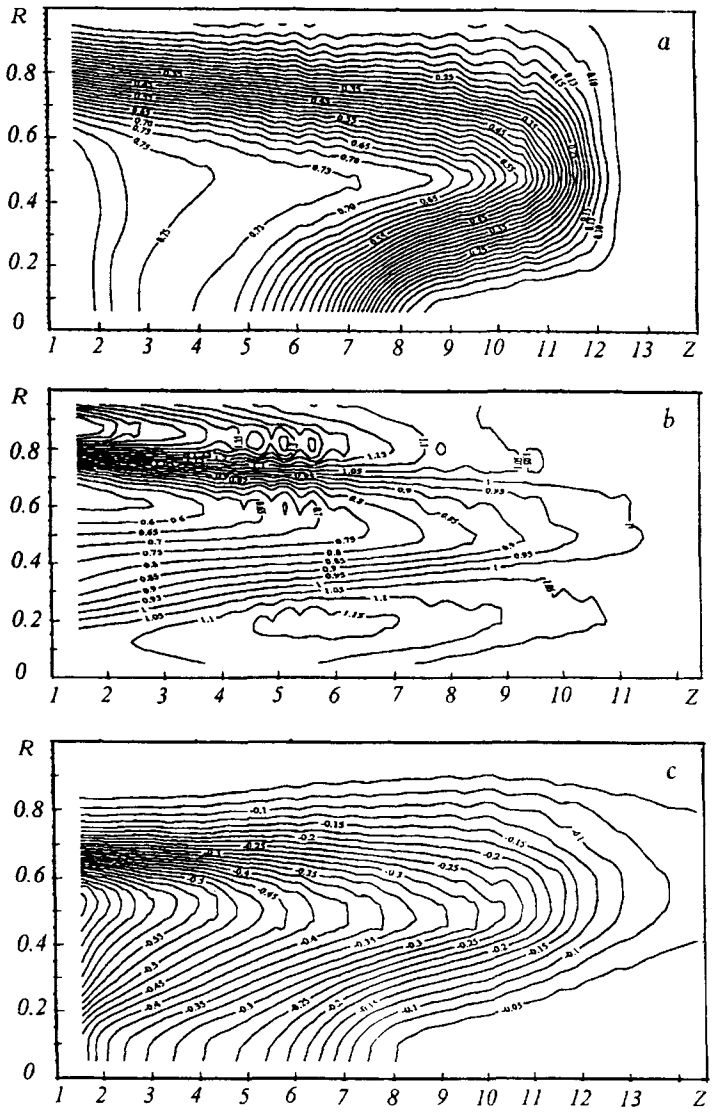

Fig. 9. Isolines of temperatures (a), densities (b), and the axial component of the radiative flow density (c) (third version). ρ, 10^{-6} g/cm^3.

The studies conducted indicate a correspondence of the chosen physical and mathematical model to the actual processes occurring in hypersonic gas flows past cosmic bodies upon their entry into the atmosphere.

The work was carried out under the program of the International Science and Technology Center, project B23-96.

NOTATION

t, time; r and z, radial and axial coordinates; $\mathbf{w} = \{v, 0, u\}$, velocity of the flow of plasma with radial, azimuthal, and axial components, respectively; E, total specific energy of the plasma; P, pressure; ρ, plasma density; ε, specific internal energy of the plasma; S, density of the radiative-energy flow.

REFERENCES

1. V. A. Bronshten, *Physics of Meteoric Phenomena* [in Russian], Moscow (1981).
2. A. V. Dobkin, T. V. Loseva, I. V. Nemchinov, et al., *Prikl. Mekh. Tekh. Fiz.*, **34**, No. 6, 35-45 (1993).
3. O. M. Belotserkovskii and Yu. M. Davydov, *Method of Large Particles in Gasdynamics* [in Russian], Moscow (1982).

4. V. E. Okunev and G. S. Romanov, in: *Heat Transfer under the Action of Radiative Flows on Materials* [in Russian], Minsk (1990), pp. 77-98.
5. G. S. Romanov, Yu. A. Stankevich, L. K. Stanchits, and K. L. Stepanov, *Int. J. Heat Mass Transfer*, 38, No. 3, 545-551 (1995).
6. B. N. Chetverushkin, *Mathematical Simulation of Problems of the Dynamics of an Emitting Gas* [in Russian], Moscow (1985).